

Automotive Science and Engineering

Journal Homepage: ase.iust.ac.ir



Design modification of shifting blocker of vehicle gearbox for strength improvement

Milad Arianfard¹, Abbas Soltani^{2*}

¹Department of Mechanical Engineering, National University of Skills (NUS), Tehran, Iran.

²Department of Industrial, Mechanical and Aerospace Engineering, Buein Zahra Technical University, Qazvin, Iran.

| ARTICLE INFO | ABSTRACT | | |
|--|--|--|--|
| Article history: Received: 19 Jan 2024 Accepted: 30 Mar 2024 | In this paper, the strength improvement of the gear shifting blocker is investigated for the Peugeot gearbox and design modifications of the part are proposed based on the customer feedback regarding its failures. A hardened steel sheet is used inside the plastic part of the shifting blocker | | |
| Published: 20 May 2024 | to increase the strength. In this research, two proposed correction designs are presented to decrease the stress of plastic part by modifying on the | | |
| Keywords: Strength improvement Gear shifting blocker | steel sheet geometry. ABAQUS software is used for modeling the gear shifting blocker and analyzing the stress distribution of the parts by finite element method. In order to validate the simulation results and choose | | |
| Fork Finite element analysis | the proper design to enhance the strength of blocker part, some experimental tests are performed on the tension-compression test bench. | | |
| Abaqus software | By comparison of the results, from both tests and simulations, it can be observed that the first and second modification designs improve the stresses of blocker plastic part by 18% and 45%, respectively. | | |

1. Introduction

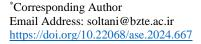
The vehicle gearbox is used for transmitting the engine power to the wheels. Gearboxes are designed based on the torque and speed of engine that is imported via input shaft. Design of each part is important based on its application and its effect on drive train. Breaking or failure of each part can cause irreparable damage to the gearbox and even the vehicle.

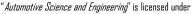
Some parts of the vehicle gearbox, such as gears, shafts, and bearings, are directly involved in power transmission, and some parts are used as safety parts to prevent improper performance or undesired actions. One of the parts of the gearbox is known as gear shifting blocker. This part is installed on the gear shift lever as a part of gear shift mechanism in such a way that it is locked inside the gearbox housing and prevents simultaneously engaging of other gears when gear shifting. This operation is carried out by placing a

number of gear shift finger parts in front of the driving part of the forks to prevent them from moving.

During shifting, the shifting finger may be located between two forks that causes two gears to be engaged simultaneously. This situation may also occur when the driver's hand is in the incorrect position on the gear shift knob. To prevent this undesired action, the gear shifting blocker part inhibits the engagement of more than one gear, and prevents the damage of the gearbox. At this moment, the driver increases the force on the fork and therefore, some zones of blocker are broken so that the mechanism loses its function.

Stress analysis of gearbox has been performed in various researches. Xiaoan Tang analyzed and investigated the stresses applied to the gearbox housing in Abaqus software and concluded the high reliability of gearbox housing and, as a result, its potential for optimizing [1]. In another





a Creative Commons Attribution-Noncommercial 4.0



research, Babu and his co-workers analyzed the stress in a single-speed gearbox in ANSYS and proposed three optimization software including changes methods. in geometry, materials, and both [2]. Also, Saritas and et al. evaluated the static stresses in the housing and gears of a three-step reduction gearbox by using ANSYS software. In addition, they obtained the natural frequencies of the gearbox and compared them with the excited frequencies in order to prevent the resonance phenomenon [3].

The internal parts of the gearbox have also been analyzed from the stress point of view. The static analysis and natural frequencies of gear shift forks has been carried out by Qiangwei [4]. In another study, Xiakan presented a three-dimensional mathematical modelling of the gear shift forks in Pro Engineer software, and then investigated and optimized the model in ANSYS utilizing the finite element method (FEM) from the stress and deformation point of view [5]. The gears are one of the important parts to transmit the power as the most important duty of gearbox and several researches have been performed about them. In this regard, stress distribution analysis has been presented using the nonlinear FEM for two simple identical gears in the most critical situation of gear contact and the obtained results have been compared with the results of Lewis, Hertz and AGMA relationships [6].

A finite element model was created for the vehicle gearbox using NASTRAN software, which presented the results of the modal analysis of the gearbox housing by numerical method. In addition, the stress distribution of the gearbox housing was investigated by applying the dynamic loads on the bearings [7].

In 2015, Makhija and his co-workers proposed an optimal design of a powertrain with a planetary gearbox based on the stress analysis of all system components by the FEM [8]. In 2018, another investigation was conducted to analyze the stress of the gearbox housing of a high-speed train based on the FEM using ANSYS [9]. In addition, another study was presented for the analysis of dynamic stresses of the gears of machines and mining equipment. Random loads were also included in this research [10].

A model of forced vibrations in a planetary gearing based on the finite element and superelement method was proposed. This model was used to solve static and dynamic problems for mechanisms with planetary gearings [11]. A three-dimensional finite element model was established by using SolidWorks and the effect of an external load distribution along the gear tooth

width was added according to actual working situations. In the SolidWorks/Simulation module, the contact relation was established based on the real assembly relations, and to calculate Von Mises stress, on the teeth. Through modal teeth frequency was analysis, the gears investigated contrastively with the inherent model of the transmission and analyzed the influence of them. The experiment was performed in the selfmade gearbox fatigue test bed [12].

Finite element analysis was applied on thermal structures of heavy machinery gearboxes. The steady-state temperature distribution of the gearbox housing was obtained by thermal structural coupled analysis. Thermal load is a significant factor to control the gearbox housing deformation to ensure the accuracy and reliability of heavy transmission systems [13]. In another research, the mechanical behavior of a single edge bonded composite plate repaired with 1-ply and 4ply composite patches was studied using the FEM. The effect of the adhesive epoxy film, patch material, thickness and ply orientations on the evolution of the stress intensity factor of the repaired structure was examined. It was concluded that shear strength and thickness of the adhesive bond are the largest factors in the effectiveness of patch repair [14].

Also, the researchers carried out the analysis, prediction and optimization of static and dynamic behavior of one type wind turbine gearbox. The static analysis results of the housing, spline and gear pairs of the gearbox were obtained using FEM and the natural frequency and modal shape of the gearbox were investigated. modification data of the flank shape for each class tooth alignment and tooth profiles were found from the analysis. Finally, the related data on the strength and stiffness of all the parts in the wind turbine gearbox were provided [15]. The gearbox for a wind turbine should be designed to have the sufficient structural strength to retain the extreme torque and forces transferred from rotor blades. Traditionally, the structural analysis of gearbox has been made using the simplified FEM models in which the contacts between gear teeth are replaced with the equivalent forces acting on the gear shafts, because the consideration of the detailed internal gear transmission system requires a huge number of degrees of freedom. But, the traditional method can neither accurately reflect the gear transmission forces, nor is it better for the dynamic analysis. In order to solve these structural analysis problems, a method considering the tooth contact of the internal gear system was presented. The actual tooth contact between a pair of gears was modeled with spring

elements and the spring constants were determined through the stiffness analysis of gear teeth. The current analysis technique was established using the comparison with the simplified gear system model and applied to the structural analysis of a 2-stage differential-type gearbox for wind turbines [16].

A new nonlinear finite element model was proposed in the framework of Carrera's Unified Formulation for the dynamic analysis of hybrid composite plates considering the instantaneous phase transformation and material nonlinearity effects, for every point on the plate. A transient FEM beside an iterative incremental procedure is studied to investigate the dynamic response of multilayered composite plates and a suppressed vibration of the plate was observed, which was due to the energy dissipation of the system [17]. In this regard, the finite element analysis of free vibration of the delaminated composite plates with variable kinematic multilayered plate elements was presented [18].

optimal design of a biodegradable functionally graded materials (FGM) composite bone plate was studied to achieve successful healing and union of bone fractures. Four design parameters of a bone plate including the average Young's modulus, spatial distribution of the FGM layers, degradation rate of the material, and thickness were varied to analyze their influences on healing of fractured bones. The design of experiments and the Taguchi method for the optimal design of the bone plate were considered. To optimize the design parameters of the bone plate and maximize the healing performance, signal-to-noise ratio was used, as a larger signalto-noise ratio was better [19]. A stochastic extended finite element method was developed for the fracture analysis along with reliability analysis of the central cracked laminated composite plate subjected to uni-axial tension with random system properties [20].

The low-velocity impact responses of cross-ply composite plates were investigated experimentally and were simulated using the finite element code LS-DYNA. An experimental test was initially performed and two different modeling methods were then applied to model the composite plates. In the first numerical modeling approach, solid elements were used for the composite layers, whereas in the second, shell elements were utilized. The numerical model using the shell elements showed a perfect correlation with the experimental results, while the impact damage in the form of delamination was predicted more exactly using solid elements [21]. In addition, a

novel adaptive high dimensional model representation was developed for stochastic finite element analysis of composite plate [22].

An investigation was performed to design and analyze triple deduction helical gearbox housing through FEM. To start with, the studies were conducted to examine and interpret the structural performance of gearbox casing. The modal and vibration analysis, harmonic analysis and response spectrum analysis were performed for existing helical gearbox casing and modified design to predict behavior of gearbox housing subjected to respective loading and no loading conditions [23].

The strength improvement of the parts for the industries related to aerospace, automotive, etc. such as the gearbox, engine and turbine using FEM is of great importance. This increases the reliability and by preventing the re-production costs, reduces the product prices. Therefore, the presented approach of this paper for enhancing the strength of gear shifting blocker can be broadly applied in the mentioned industries. These methodologies are not usually similar in different case studies due to differences in geometry, material and application.

In this paper, the strength of the plastic part of the gear shifting blocker for the Peugeot gearbox is investigated. A CK45 steel sheet is inserted into the mold in the plastic injection machine in order to increase the strength of this part. The sheet metal is adhered to plastic and increases the strength. The contributions of the study can be listed as follows:

- Two modified designs are proposed to improve the strength of the plastic part by modifying the geometry of steel sheet using the FEM based on ABAOUS software.
- The experimental tests are carried out for validating the FEM model and very close agreement between test and simulation results are obtained after model updating.

2. Finite element modeling of the gear shift blocker

In this section, first, the gear shifting blocker part is modeled by FEM in ABAQUS software. For this purpose, the 3D model is imported from CATIA Software. Then in ABAQUS, the shifting force and boundary conditions are applied on the part.

2.1. Definition of materials

In various industries such as automotive engineering, the parts are usually made using plastic, metal or combination of both and composite materials. The main targets of material selection are reducing weight and increasing strength. To decrease the weight, plastic materials and to increase the strength, metallic materials are preferred. The composite materials fulfill both aims together.

Definition In ABAQUS, of polyamide reinforced with 30% glass fiber as material is another step of modeling. Due to the combination of glass fiber and plastic homogeneously in this part, the material is considered as a composite. But regarding the distribution of glass fiber in the plastic homogeneously, the properties of combined material can be considered as a unique material with no changes in different directions. The steel sheet is also defined in this software. The properties of the mentioned material can be seen in Tables 1 and 2.

Table 1: Mechanical properties of the plastic part of PPA6.6- GF30 [24]

| Properties | Unit | Value |
|--------------------------------------|-------|-------|
| Modulus of Elasticity | МРа | 5700 |
| Modulus of Elasticity in Compression | МРа | 4100 |
| Tensile Strength | МРа | 98 |
| Yield Strength | МРа | 98 |
| Impact Strength | KJ/m² | 97 |

Table 2: Mechanical properties of the steel sheet of CK45

| Properties | Unit | Value |
|-----------------------|------|-------|
| Modulus of Elasticity | GPa | 206 |
| Yield Strength | МРа | 450 |
| Ultimate Strength | МРа | 585 |
| Fracture Strain | % | 12 |
| Poisson's Ratio | - | 0.29 |
| | | |

2.2. Definition of Connection Points

In this section, both parts should be connected to each other according to the production conditions. Due to injection of hot melt plastic in the mold, the sheet metal and plastic will almost stick to each other. In ABAQUS, the "Tie" option is used for this purpose, so that the displacement of the points that are in contact with each other in two adjacent parts is considered the same. Two mentioned parts are shown in Figure 1.

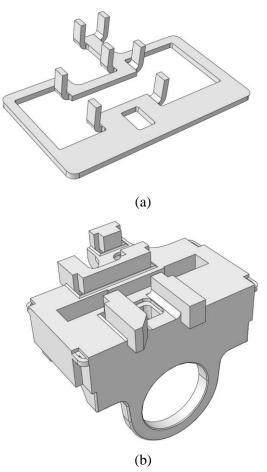


Figure 1: (a): Insert sheet part of blocker, (b): Plastic part of blocker

2.3. Load

In order to evaluate the stresses of the part under the shifting force, the boundary and force conditions are defined and applied as follows. The force of 360 N is applied as an input to this part. This value has been obtained according to the gear shifting forces.

Fixed boundary conditions have been considered for two sides of the blocker part, which is actually locked inside the gearbox housing. The type of applied force and the boundary conditions are shown in Figure 2.

2.4. Meshing

One of the most important steps of this analysis is meshing. Meshing is converting complex parts into small elements and simplifying equations based on FEM. The type of meshing for this part is C3D4 with linear distribution, a 4-point tetrahedral mesh, which is used for relatively complex parts.

Although, there is a limitation for this type of mesh which is the angle of the mesh corners that should not be less than 6 degrees. The size of the mesh grids for this part is 1.5 mm, which is reduced to 0.5 mm in critical points such as corners and the region of applying the force and in the area of failure. The number of elements of this part is 88072 and average of its shape factor is 1.83, which indicates the appropriate quality of the mesh for this part.

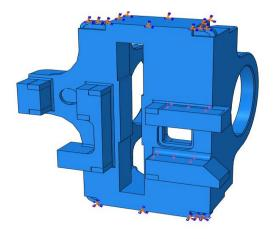


Figure 2: Boundary conditions for plastic part of blocker

3. Simulation results of the FEM

By applying the boundary conditions, loading and meshing of the part, the von Mises stress distribution can be seen as follows for both parts in Figures 3 and 4. In most of static analysis, the Von Mises Stress is often used to determine the condition of part under the static loads.

$$\sigma_{eq} = \begin{cases} 0.5[(\sigma_{x} - \sigma_{y})^{2} + (\sigma_{y} - \sigma_{z})^{2} \cdots \\ \cdots + (\sigma_{z} - \sigma_{x})^{2}] + 3(\tau_{xy}^{2} + \tau_{yz}^{2} \cdots \\ \cdots + \tau_{zx}^{2}) \end{cases}$$
(1)

where σ_x , σ_y and σ_z are the main stresses and τ_{xy} , τ_{yz} and τ_{xz} are the component of three-dimensional stresses [12].

The Von Mises Stress equation can be written as expected in this type of composite parts, a percentage of the stresses is borne by the plastic part and the other share by the steel part. Therefore, the purpose of the design is that the steel part and the plastic part should sustain more and less stresses due to their endurance limits respectively.

As mentioned earlier in Table 1, the yield stress of the plastic part is 91 MPa and for the steel part is 450 MPa. As an accepted principle, The Factor of Safety (FS) is the ratio of the actual

strength of a structure (ultimate stress) to the maximum stress it should sustain in service (allowable stress). It is a measure of how much stronger a system is than it needs to be for a corresponding intended load. So, by reducing the amount of stress in the plastic part, by keeping constant the material strength, the safety factor of this part will increase. Therefore, in the next section, two suggestions are presented to reduce the stress in the plastic part and increase its safety factor.

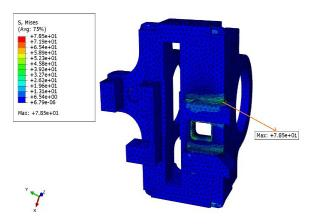


Figure 3: Stress contour for plastic part of primary blocker

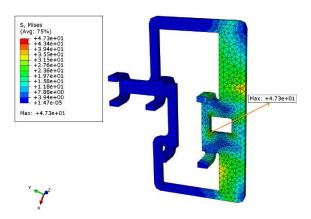


Figure 4: Stress contour for metallic insert part of primary blocker

4. Presenting the corrective plans

In this section, two plans are proposed to modify the plastic part in order to increase its safety factor.

4.1. First suggestion plan

In the first plan, which is implemented on the insert part, two slots are created on the steel part. It is expected the stress flow is transmitted from the plastic part to the steel part by connecting two sides of the plastic to each other and also locking the steel part in itself. Considering that the steel

part bears more stress in comparison with the plastic part, the safety factor of the plastic part will increase. The finite element modeling of this part is also performed with the same conditions as the primary part in ABAQUS. The results of its stress distribution can be depicted in Figures 5 and 6. So as it is observed from Figures 5 and 6, the maximum stress is decreased in plastic part and is increased in steel part in comparision to Figure 3 and 4, respectively.

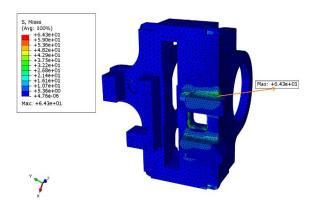


Figure 5: Stress contour for plastic part of blocker-first proposed design

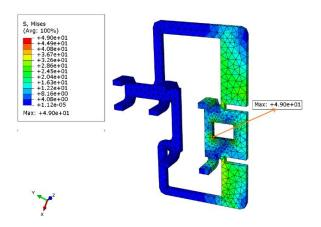


Figure 6: Stress contour for sheet insert part of blocker - first proposed design

4.2. Second suggestion plan

In the second correction, a slot is created on the steel part and then it is bent. This bent sheet can withstand the force and prevent the stress to transfer to the plastic part and also the plastic part is stuck to each other on both sides of the steel part. Due to the adhesion of the two parts, its endurance is increased. The applied stresses of the blocker for the second suggestion can be illustrated in Figures 7 and 8.

According to the results obtained from the diagrams in Figures 7 and 8 and the given explanations, it seems that the second proposed

plan can significantly reduce the stress on the plastic part and prevent it from failure. In Table 3, the stress in the initial part, in the parts with the first and second suggestions and its improvement percentage as well as their safety factor based on the yield stress of the plastic part are given.

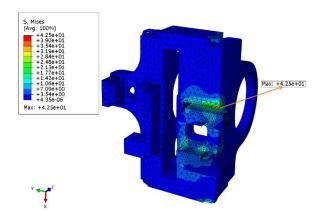


Figure 7: Stress contour for plastic part of blockersecond proposed design

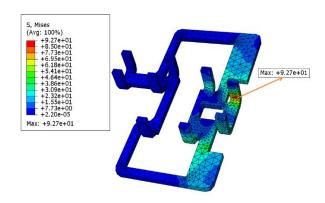


Figure 8: Stress contour for sheet insert part of blocker-second proposed design

Table 3: FEM results of the blocker part

| Parts | Maximum of stress for plastic part | Maximum of stress for steel part | Safety factor for plastic part | Improvement percentage of stress for plastic part |
|-----------------------------|---|--|---|--|
| Initial Part | 78 MPa | 47 MPa | 1.25 | 0 % |
| First Suggested Plan | 64 MPa | 49 MPa | 1.53 | 17.8 % |
| Second Suggested Plan | 43 MPa | 93 MPa | 2.27 | 44.8 % |

As it is observed from table 3, the first suggested plan gave us 17.8% reduction in plastic stress and in second one, by creating some bend in the steel sheet and by translating the stress from plastic part to metal sheet, the stress in plastic part reduced 44.8% in comparison to initial part. This

is useful because the sheet metal has more durable material than plastic part.

5. The results of experimental tests

In order to validate the analytical results and choose the appropriate design to increase the blocker strength, several experimental tests were performed on the tension-compression test machine. This device consists of a mechanism of applying the force, a load cell and a force display gauge. After designing and building a fixture for installing the part, it has been used as a test device for this part in the laboratory. This fixture is shown in Figure 9.

These tests were carried out on 4 samples of the current parts, 4 samples of the first proposed part and 4 samples of the second proposed part. The load is applied on the part until it fails. When the failure occurred, the amount of force was read from the force display gauge and recorded. The results of the tests can be seen in Table 4.

Table 4: Experimental results of the blocker part

| Part No. | Blocker part | Failure force (N) | Average of Failure force (N) | Improvement percentage of Failure force | |
|-------------|--------------|----------------------|------------------------------|---|--|
| 1 | Initial Part | 330 | _ | 0 % | |
| 2 | Initial Part | 321 | - 323 | | |
| 3 | Initial Part | 335 | _ 323 | | |
| 4 | Initial Part | 306 | _ | | |
| 5 | First Plan | 377 | _ | 15.2 % | |
| 6 | First Plan | 360 | - 372 | | |
| 7 | First Plan | 371 | - 3/2 | | |
| 8 | First Plan | 380 | _ | | |
| 9 | Second Plan | 464 | | 20.2.0/ | |
| 10 | Second Plan | 433 | 450 | | |
| 11 | Second Plan | 448 | - 450 | 39.3 % | |
| 12 | Second Plan | 455 | = | | |

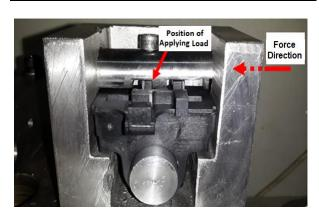


Figure 9: Fixture for test of locker part

The comparison of results between FEM and experimental tests about the percentage of improvement related to two suggested plans can be shown in Figure 10.

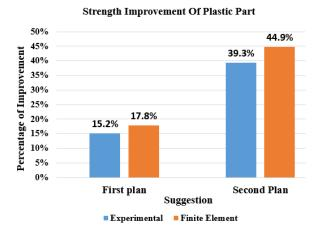


Figure 10: Comparison of results between FEM and experimental tests

As it was expected from FEM results, the result of experimental were almost similar to FEM. The first and second plans increased the factor of safety to 15.2% and 39.3% respectively. The sources of errors between FEM and tests and also the uncertainties in experimental validation depend on several items such as mesh sizing, differences between actual and theoretical material properties, errors in fabrication of test fixture, frictional behavior of fixture, load cell accuracy, etc.

6. Conclusion

According to the simulation results from the FEM analysis as shown in Table 3, it can be concluded that the first and second modification designs enhance stresses of the blocker plastic part by 18% and 45%, respectively. In addition, as depicted in Table 4, the experimental tests indicate that the failure force in the corresponding part is increased by 15% and 39%, respectively. Comparing the above results, it can be seen the small difference between the simulation and test results. This error is due to the quality of mesh, solver accuracy, experimental machines and test facilities. Although, the small amount of error can be ignored in comparison with the great improvement in strength.

There are still some problems to be further studied in choosing the plastic with higher strength and lower weight so that there is no need to insert a metal sheet. This research can be expanded by replacing composite materials instead of utilizing plastic and metal materials together. Also, this study may be explored in

future through applying several methods of optimizing the geometric design features such as geometric form optimization (topology optimization) and dimension values (parametric optimization).

References

- [1] X. Tang. Structural strength analysis of gearbox casing based on ABAQUS. InIOP Conference Series: Materials Science and Engineering, IOP Publishing, Dec 1, Vol. 677, No. 5, (2019), p. 052067.
- [2] M. Babu, Y. Reddy, Stress analysis of gearbox casing using anys workbench. Applied Research and Technology, Vol. 8, (2016), pp. 1397-1405.
- [3] M. Saritas, O. Golbol, P. Yayla. Finite element stress analysis of three-stage gear box. Niğde Ömer Halisdemir University Journal of Engineering Sciences, Vol. 10, No.2, (2021), pp. 784-790.
- [4] L. Qiangwei. Finite element analysis and vibration control of lorry's shift mechanism. InIOP Conference Series: Materials Science and Engineering, IOP Publishing, Nov 1, Vol. 269, No. 1, (2017), p. 012010.
- [5] Z. Xiaokun. Optimization design and fracture analysis of shift fork shaft of the transmission. International Conference on Advanced Technology of Design and Manufacture (ATDM), (2011), pp. 1-3.
- [6] T.N. Chakherlou, M. Abdi. Contact stress analyses for spur gear teeth. 14th Annual-International Conference on Mechanical Engineering, Isfahan University of Technology, Isfahan-Iran, (2006), May 16-18.
- [7] R. Dai, J.S. Ma, H.D. Zhang. Modal and strength analysis on a gearbox housing. Advanced Materials Research Journal, Vol. 154, (2011), pp. 1379-1383.
- [8] G. Makhija, M. Mahajan, N. Bansod, S. Bakshi. Design and optimization of powertrain using hybrid planetary gearbox for formula student vehicle. InInternational Design Engineering Technical Conferences and Computers and Information in Engineering Conference, American Society of Mechanical Engineers, Aug 2, Vol. 57205, (2015), p. V010T11A055.

- [9] Z. Wang, G. Mei, W. Zhang, Y. Cheng, H. Zou, G. Huang, F. Li. Effects of polygonal wear of wheels on the dynamic performance of the gearbox housing of a high-speed train. Proc. IMechE, Part F: J. Rail and Rapid Transit, Vol. 232, No. 6, (2018), pp. 1852-1863.
- [10] R. Zhang, Y. Zhang. Dynamic characteristics for coal shearer cutting unit gearbox housing. Mechanics & Industry Journal, Vol. 21, No. 2, (2020), pp. 1-21.
- [11] A.I. Bednyi. Mathematical simulation of epicycle gear vibrations in a planetary gearbox using finite element analysis. Journal of Machinery Manufacture and Reliability, Vol. 36, No. 5, (2007), pp. 425–429.
- [12] T. Jin, L. Yaoming. Finite element analysis of input gears in a gearbox of combine harvester. Fourth International Conference on Intelligent Computation Technology and Automation, IEEE, Vol. 2, (2011), pp. 77-80.
- [13] Y. Mei, F.P. Wang, Q.Y. Liu, Y.T. Mao. Finite element analysis on thermal structures of heavy machinery gearbox. Advanced Materials Research, Vol. 228, (2011), pp. 651-655.
- [14] L. Gu, A.R. Kasavajhala, S. Zhao. Finite element analysis of cracks in aging aircraft structures with bonded composite-patch repairs. Composites, Part B: Engineering, Vol. 42, No. 3, (2011), pp. 505-510.
- [15] W. Jing, X.J. Sun, W. Sun, A.G. Guo. Finite element analysis of the static/dynamic behavior of wind turbine gearbox. Applied Mechanics and Materials, Vol. 187, (2012), pp. 138-145.
- [16] J.R. Cho, K.Y. Jeong, M.H. Park, D.S. Shin, O.K. Lim, N.G. Park. Finite element structural analysis of wind turbine gearbox considering tooth contact of internal gear system. Journal of Mechanical Science and Technology, Vol. 27, (2013), pp. 2053-2059.
- [17] S.M. Khalili, M.B. Dehkordi, E. Carrera. A nonlinear finite element model using a unified formulation for dynamic analysis of multilayer composite plate embedded with SMA wires. Composite Structures, Vol. 106, (2013), pp. 635-645.

- [18] S.K. Kumar, M. Cinefra, E. Carrera, R. Ganguli, D. Harursampath. Finite element analysis of free vibration of the delaminated composite plate with variable kinematic multilayered plate elements. Composites, Part B: Engineering, Vol. 66, (2014), pp. 453-465.
- [19] H. Mehboob, S.H. Chang. Optimal design of a functionally graded biodegradable composite bone plate by using the Taguchi method and finite element analysis. Composite Structures, Vol. 119, (2015), pp. 166-173.
- [20] A. Lal, S.P. Palekar, S.B. Mulani, R.K. Kapania. Stochastic extended finite element implementation for fracture analysis of laminated composite plate with a central crack. Aerospace Science and Technology, Vol. 60, (2017), pp. 131-151.
- [21] F. Ahmad, F. Abbassi, M.K. Park, J.W. Jung, J.W. Hong. Finite element analysis for the evaluation of the low-velocity impact response of a composite plate. Advanced Composite Materials, Aug 30 (2018).
- [22] A.K. Rathi, A. Chakraborty. Development of hybrid dimension adaptive sparse HDMR for stochastic finite element analysis of composite plate. Composite Structures, Vol. 255, (2021), 112915.
- [23] R.D. Gandhi, N.S. Patel. Design, analysis and modification of 3 stage helical gearbox casing using finite element method considering different materials. In Proceedings of International Conference on Intelligent Manufacturing and Automation: ICIMA 2018, Springer Singapore, (2019), pp. 99-114.
- [24] https://www.ensingerplastics.com/en/shapes/products/pa6-tecamid-6-gf30-black